Desalination and Water Treatment
www.deswater.com

doi: 10.5004/dwt.2017.21612

97 (2017) 295–303
November

Chitosan anchored zinc oxide nanocomposite as modified electrochemical sensor for the detection of Cd(II) ions

G. Padmalaya[a], B.S. Sreeja[a,*], P. Senthil Kumar[b,*], M. Arivanandhan[c]

[a]*Department of Electronics and Communication Engineering, SSN College of Engineering, Kalavakkam, India, Tel. +91 9790915273; email: sreejabs@ssn.edu.in (B.S. Sreeja), Tel. +91 9841255826; email: padmalayag@ssn.edu.in (G. Padmalaya)*
[b]*Department of Chemical Engineering, SSN College of Engineering, Kalavakkam, India, Tel. +91 9884823425; email: senthilchem8582@gmail.com*
[c]*Centre for Nanoscience and Technology, Anna University, Chennai, India, Tel. +91 7401182819; email: arivucz@gmail.com*

Received 30 August 2017; Accepted 8 November 2017

ABSTRACT

The chitosan anchored zinc oxide nanocomposite (NC) has been prepared using chemical approach. The obtained NC was used as modified electrode for selective detection of Cd(II) ions using square wave voltammetry under pH 6 phosphate buffer solution. Surface area and porous nature of NC were found by using Brunauer–Emmett–Teller isotherm analysis. The presence of functional groups was confirmed using Fourier transform infrared spectroscopic analysis. The results indicated that detection starts at 30 s with least concentration along with rise in peak current and optimized potential at 0.6 V. Upon increasing the ionic concentration, intensity of the current peaks decreases due to strong porous nature of the obtained product disturbing electron transport. Under optimal conditions, the calibration plot for Cd(II) is found to be linear with concentration range of 0.2–1.5 μM and also compared with calibration plot with accumulation time. Combining the high surface area, more active sites, and reduction in particle size the absorption ability toward Cd(II) ions was found to be fast and sensitive with limit of detection 1.39 nM. Hence, the obtained product shows adequate sensing drive and it can also be used for real-time analysis.

Keywords: Chitosan; Zinc oxide nanoparticles; Current; Peak response; Cadmium ions; Electrochemical sensor

1. Introduction

The significance of heavy metals detection has expanded immensely in recent decades because of their harmfulness to human beings and animals even at low concentrations. Cadmium is found to be one of the harmful and carcinogenic to humans and its exposure leads to cardiovascular disease, cancer mortality, and damage to liver and kidneys [1–4]. Several analytical systematic procedures such as flame atomic absorption spectroscopy [5], atomic absorption spectrometry [6], and inductively coupled plasma atomic emission spectrometry [7] were used but they are more expensive, require long analysis times and suffer in operational difficulties. There is a current dynamic try to build up a detection ways to deal with heavy metal contamination with electrochemical technique which is outstanding because of its numerous ideal conditions such as time consuming, minimal effort, and high sensitivity for making the decision of detecting heavy metals.

Previously, the noble metals such as gold (Au) [8–10] and silver (Ag) [11] were used as modified electrochemical sensing material due to their high reproducibility, stability, and better electroanalytical performance in various applications. But these noble metals are quite costlier and the usage also limited. In order to overcome this scenario, recent research was intended to focus on metal oxides which are capable of providing feasible platforms due to their strong stability and

* Corresponding author.

amazing effects. The surface modifications with polymers over these metal oxides afford extra advantages of water compatibility toward the targeted specific ions. In addition, polymers are lightweight, low-cost, good processability, and efficiency [12]. Till date $MnCo_2O_4$ [13], Bi_2O_3 [14], MnO_2 [15], and CeO_2 [16] have been exposed for the electrochemical detection of heavy metals. Conductive carbon materials such as graphene and CNT are normally denoted as reasonable competitors since they are not just pad the inward anxiety instigated by volume change, yet additionally make the composites more conductive. Graphene, a two-dimensional (2D) honeycomb sp^2 carbon cross-section, has activated overall research enthusiasm for different applications due to its high surface range, great electrical conductivity, and solid mechanical stability. Recent reports based on reduced graphene oxide–Fe_3O_4 nanocomposite (NC) [17], nafion–graphene NC film [18], and nanostructured materials such as $–NH_2$ functionalized Si nanowires [19], NC incorporated in chitosan matrix [20] were pulled the specialists toward identification of heavy metal application yet the primary burden of these nanostructured materials lies in chemical instability and sensitivity. These materials are involved with simultaneous detection and these systems lack in selectivity and sensitivity. Moreover, their high-cost and complicated preparation process were confined their utilization for heavy metal detection. Therefore, it is important to develop simple and effective method for the preparation of chitosan-based NC along with satisfying the above requirements. ZnO is an environment-friendly material which has rapid research developments on major diverse applications such as sensors in food applications [21,22], photocatalyst [23], and gas sensor [24]. To the best of our knowledge, chitosan anchored (CA) zinc oxide NC has never been investigation in detection of heavy metals. In addition, chitosan is a natural polysaccharide derived from incomplete deacetylation of chitin with excellent biocompatibility, biodegradability, antibacterial property, and metal binding ability and excellent chemical stability [25–28]. According to the previous reports [28–30], bioactive molecules in the chitosan forms a hydrophilic surface interaction on the glass carbon electrode which have been utilized as sensing platform to target heavy metals. Moreover, negatively charged chitosan interacts with positively charged ZnO forming a NC for adsorbing Cd(II) ions and thus forms the sticky adherence on the electrode surface. Therefore, it is highly essential to prepare the CA ZnO NC for effective detection of Cd(II) ions.

In this paper, CA ZnO NC was prepared by simple chemical approach. The NC was used as electrode material for detecting Cd(II) ions. The sensing toward Cd(II) provides good adsorption ability, selective sensing capability, and good chemical stability due to the functionalization of chitosan and thus provided the sensitive electrochemical platform of determination of Cd(II) ions.

2. Experimental

2.1. Materials

Zinc acetate dihydrate ($Zn(CH_3COO)_2{\cdot}2H_2O$, 99.5%) and sodium hydroxide (NaOH, 97%) was purchased from Fisher Scientific (India). Chitosan ($C_{56}H_{103}N_9O_{39}$, 99%) and cadmium acetate dihydrate ($Cd(CH_3COO)_2{\cdot}2H_2O$, 98.0%) were bought from Sigma-Aldrich (India). Phosphate buffer solution (PBS) of pH 4 and 6 was obtained from Fisher Scientific. All the chemicals were used as received without further purification. Deionized water was used for all reactions.

2.2. Apparatus

Spectrum of Fourier infrared spectroscopy (JASCO FT-IR-6300, Japan) was used to analyze functional groups obtained in the product. N_2 adsorption/desorption and also pore size, surface to volume ratio measurements were carried out using Quantachrome NOVA automated gas sorption systemsorb-1.12 (Japan). Surface morphology using scanning electron microscopy (SEM) images were obtained by TESCON, Japan. All cyclic electrochemical measurements (cyclic voltammetry and square wave voltammetry [SWV]) were carried out using VMP3 computer controlled potentiostat (Bio-Logic Science Instruments, India) and performed a conventional three electrode cell with modified glassy carbon electrode (GCE) as working electrode, Ag/AgCl as counter electrode and a calomel electrode as reference electrode.

2.3. Synthesis of ZnO nanoparticles and chitosan functionalized ZnO nanocomposite

ZnO nanoparticles (NPs) was prepared by using chemical method in which 1.2 g of zinc acetate dihydrate was stirred along with 0.4 g of sodium hydroxide to obtain zinc oxide NPs [31] and to prepare the CA ZnO NC, the above ZnO NPs solution was added with 0.05 g of chitosan under vigorous stirring. This solution is further stirred for 4 h in order to obtain homogenous solution. The obtained product was centrifuged under 5,000 rpm and supernatant was washed using distilled water (DW) and dried in hot air oven at 200°C. The obtained product was used for further testing analysis.

2.4. Fabrication chitosan functionalized ZnO NPs modified GCE

The bare GCE was washed with ethanol to remove the residue at the surface and then again washed with DW finally allowed to dry. CA ZnO NC powder (3 mg) was mixed with 10 μmL of ethanol and they were allowed to sonicate till they form as homogenous ink. The obtained ink was transferred to GCE and allowed to dry at room temperature. The GCE modified electrode was used for analyzing their electrochemical behavior.

3. Results and discussion

3.1. X-ray diffraction analysis

The crystal structure of the pure ZnO NPs and CA ZnO NC was confirmed by X-ray diffraction (XRD) analysis as shown in Fig. 1. In Figs. 1(a) and (b), the diffraction peaks of ZnO NPs and CA ZnO NC were well matched with standard JCPDS no. 36-1451 which confirms wurtzite structure. Moreover, the intensity of the diffraction peaks was relatively decreased for the composite and the peaks were broadened which confirms the composite formation. The crystallite

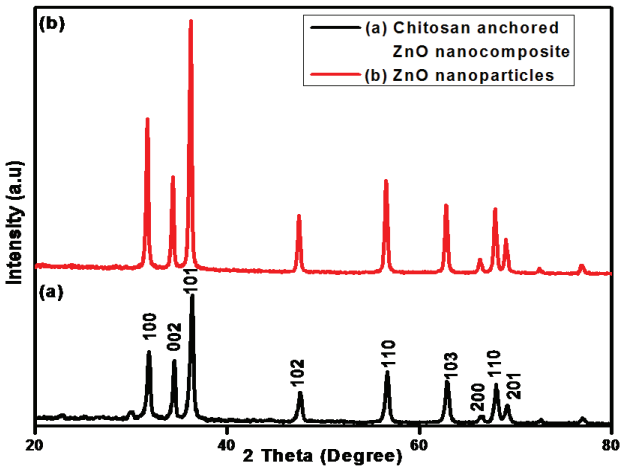

Fig. 1. XRD patterns of (a) chitosan anchored ZnO nanocomposite and (b) ZnO NPs.

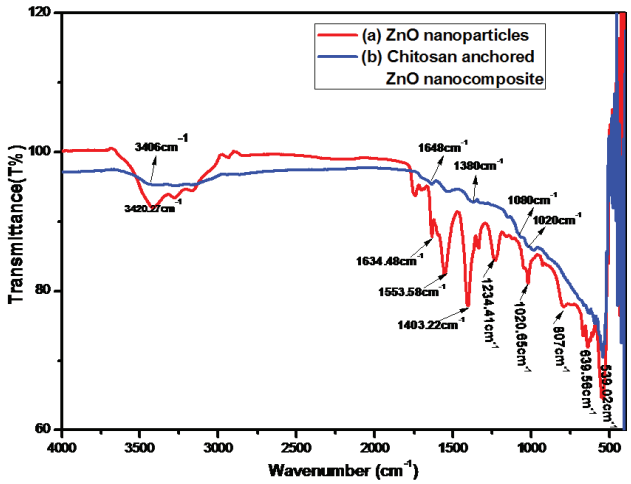

Fig. 2. FTIR spectrum of (a) ZnO NPs and (b) chitosan anchored ZnO nanocomposite.

size of the samples was calculated from XRD patterns using Debye–Scherrer formula:

$$D = \frac{0.9\lambda}{\beta \mathrm{Cos}\theta}$$

where β is the full width half maximum in radians, λ is the X-ray wavelength (1.54 Å for Cu K_α), θ is Bragg's angle in degrees.

It was observed that the diffraction peak of (101) at 2θ of 36.1 was shifted to 36.3 for the NC possibly due to the presence of chitosan. Moreover, it was found that the crystallite size decreased to 33 nm for NC compared with the size of 45.9 nm for ZnO NPs. The anchoring of ZnO with chitosan may control the agglomeration of ZnO NP and thereby the size decreased in the NC [32].

3.2. FTIR study

In order to investigate the formation of functional groups for ZnO NPs and CA NPs Fourier transform infrared spectroscopy (FTIR) was performed as shown in Fig. 2. FTIR spectrum of CA ZnO NC as shown in Fig. 2(b) provides the characteristics band at 3,406 cm^{-1} attributes to OH stretching vibration, absorption peaks at 1,648 and 1,380 cm^{-1} ascribed to bending vibration of $–NH_3$ and CH_3 symmetrical deformation mode, the band at 1,020 cm^{-1} attribute to C–O stretching vibration, respectively. The absorption band at 539.02 cm^{-1} is characteristic stretching mode of Zn–O [33]. Fig. 2(a) shows the IR spectrum of ZnO NPs provides the characteristic peak at 539.02 cm^{-1} corresponds to the formation of Zn–O. The absorption peaks at 3,420 cm^{-1} corresponds to –OH stretching vibration of water. The peaks recorded at 1,634 and 1,553.58 cm^{-1} are from C=O band, the band at 1,403.33 cm^{-1} represents carboxylate group (COO^-). The peak at 1,020 cm^{-1} depicts the stretching vibration of C–O attributed to zinc acetate. The band centered at 807 cm^{-1} is attributed to bending mode of carbonate [34,35]. On observing both the plots of FTIR spectrum, ZnO NPs when anchored with chitosan it did not affect the functional properties and structural properties almost maintained even after the anchoring process with chitosan (polymer).

3.3. Surface morphology

Figs. 3(a) and (b) show the SEM images of ZnO NPs and Figs. 3(c) and (e) show CA ZnO NC. From the SEM images of ZnO particles, it was found that the particles have spherical morphology and the particles are severely agglomerated. Figs. 3(c) and (e) show that the particles in the composite are monodispersed with no agglomeration. Moreover, particle size of ZnO anchored with chitosan is relatively small compared with that in pure sample which confirms that the presence of chitosan suppresses the agglomeration of ZnO particles.

3.4. N_2 adsorption and desorption

Fig. 4 shows linear isotherm Barrett-Joyner-Halenda plot of the NC which resembles type I isotherm which confirms particles are microporous ranging from 0 to 0.2 (IUPAC classification). This is due to the anchoring of chitosan up on the zinc oxide NPs. Further, the formed ZnO NPs provide large surface area when modified with chitosan that enhances the adsorbing process toward Cd(II) ions. Moreover, biomolecules such as amine and hydroxyl groups present in chitosan took active part in increasing the active sites for targeting metal ions. The Brunauer–Emmett–Teller (BET) surface was found to be 0.94 m^2/g and pore volume 11.79 Å. Microporous nature of the NC increases the charge–carrier transport which further decreases the peak current.

3.5. Optimization of experimental parameters

In order to get the responses of heavy metal ion influencing the voltammetric response toward Cd(II) ions includes supporting pH medium, accumulation potential, and accumulation time were optimized in aqueous solution.

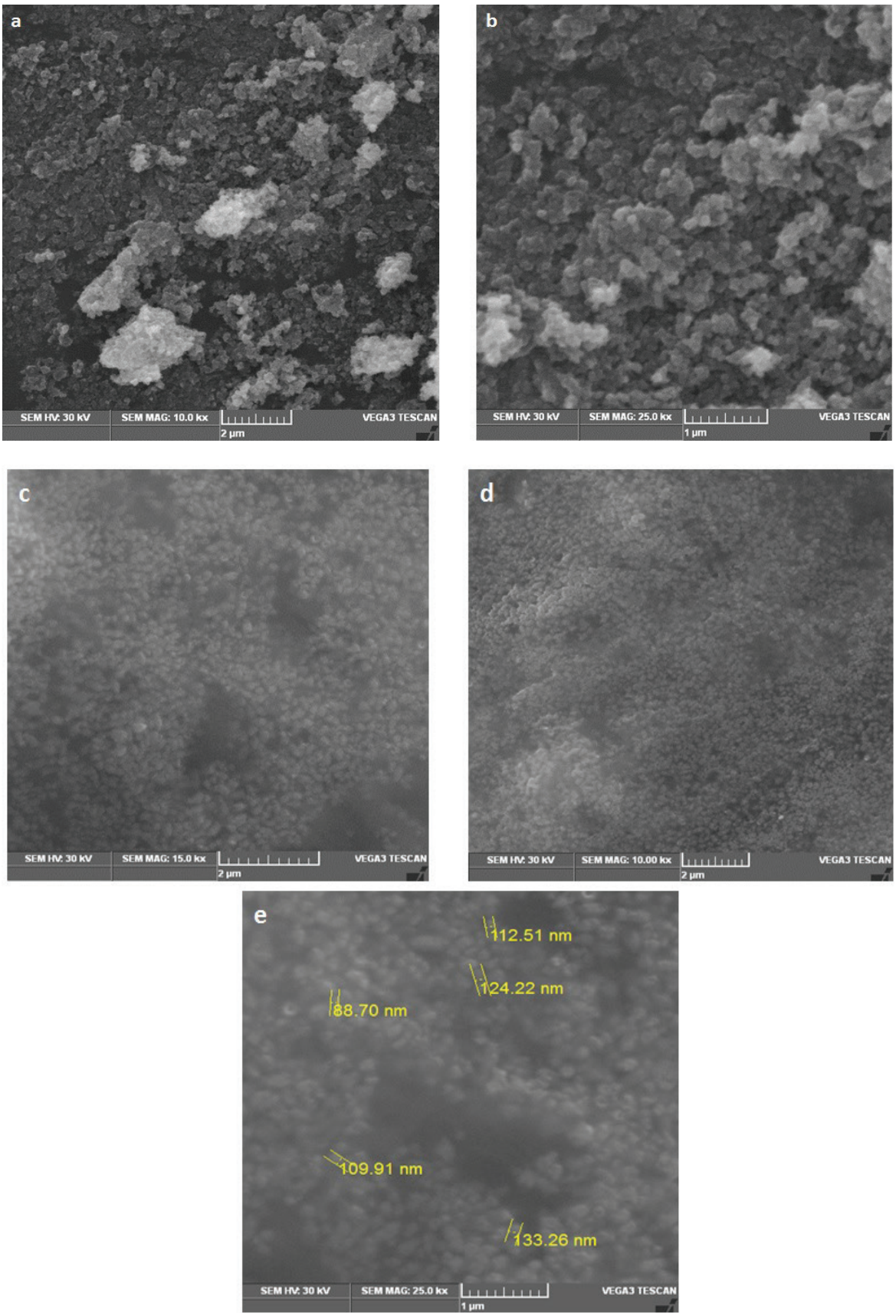

Fig. 3. SEM images of (a) and (b) ZnO NPs and (c) and (e) chitosan anchored ZnO nanocomposite.

3.5.1. Effect of pH

The strength of the stripping peaks was influenced by pH value. At about, pH 6, it was noticed that strongest stripping peak and no other stripping peaks were noticed at pH 2 and pH 4. Therefore, the supporting electrolyte of pH 6 was employed for further detection.

3.5.2. Effect of accumulation potential

Deposition potential is another important factor for achieving the best sensitive response. The deposition potential was studied in the range of 0 V to –1.0 V at 0.2 μM of Cd(II) as shown in Fig. 5(a). It can be seen that peak was gradually increasing and at –0.6 V it produced a highest current peak. However, the peak current started to decrease suddenly when it exceeds –0.7 V. As the deposition potential becoming more negative, the metals deposited on the surface of the electrode affected by hydrogen bubbles and prompted in diminishing the current peaks at very negative potentials [17].

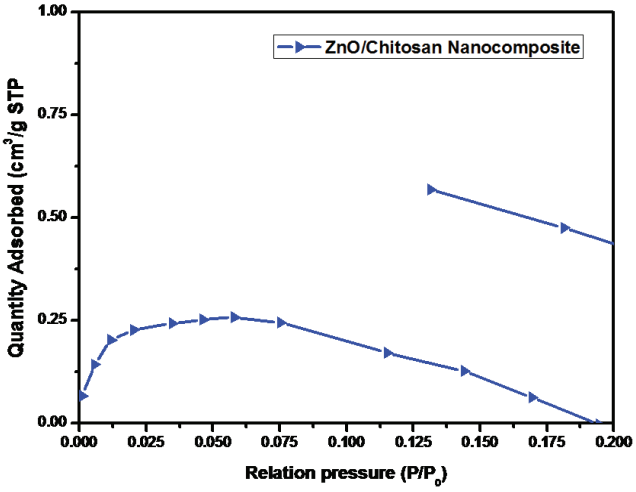

Fig. 4. BET adsorption isotherm plot.

3.5.3. Effect of accumulation time

The accumulation time is important factor that determines the detection limit and sensitivity. The accumulation time was studied in 0.2 μM Cd(II) range of 30–180 s as shown in Fig. 5(b). The stripping peaks were tending to increase with increasing the accumulation time and reached saturation after 150 s. This is due to increased concentration of analyte on the surface of the modified electrode and later gets saturated.

3.5.4. Electrochemical behavior of glassy carbon electrode modified chitosan anchored ZnO nanocomposite and its mechanism

Fig. 7 shows the SWV behavior of GCE modified CA ZnO NC toward Cd(II) ions. The obtained product shows improved current peaks at increasing concentration of metal ions. Under typical conditions, detection of Cd(II) ions was found to get better current response begins at 30 s itself and this may be due to the interaction between the NC at the electrode surface shows good affinity toward the metal ions. Moreover, the results could be adsorbing capacity of biomolecules (amines and hydroxyl) groups present in NC showed excellent attraction toward metal ions. But falling current peaks were noticed when metal ion concentration increased. This is due to the increase in pore distances, provided higher current peaks and when metal ions started to accumulate further, the porous nature becomes weak so the adsorbing capacity of metal ions on surface of modified electrode ended up with noticeably frail and occurred a diminish in current peak. Linear range for the varying concentration plot has been calculated and found to be $R^2 = 0.9429$ as shown in Fig. 7(b) which was compared with varying accumulation time plot fitted value as shown in Figs. 6(a) and (b). The stripping behavior of NC materials showed acceptable improved

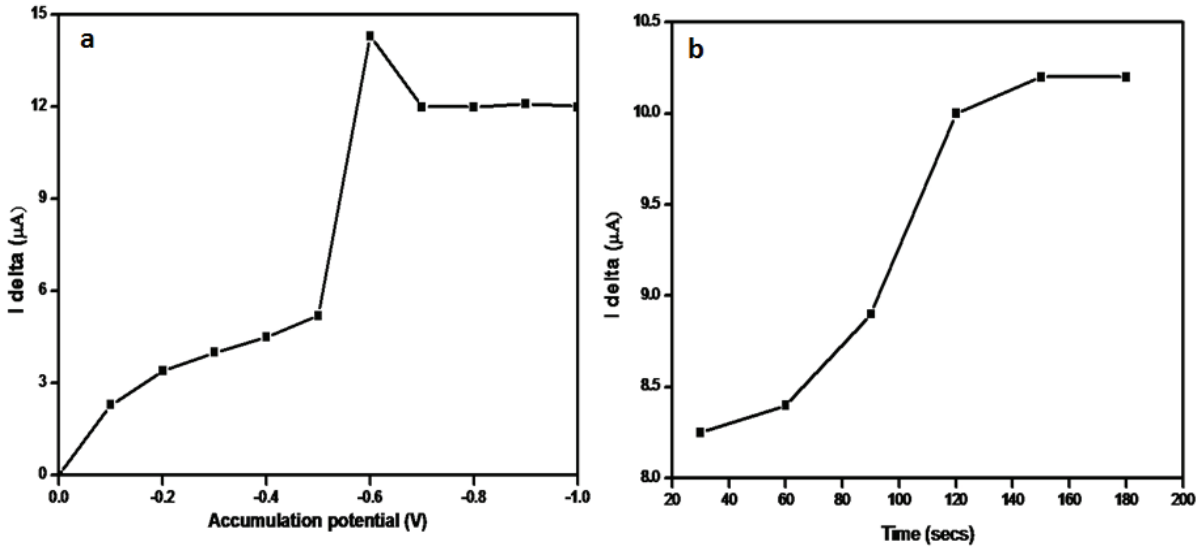

Fig. 5. (a) The effect of accumulation potential and (b) accumulation time.

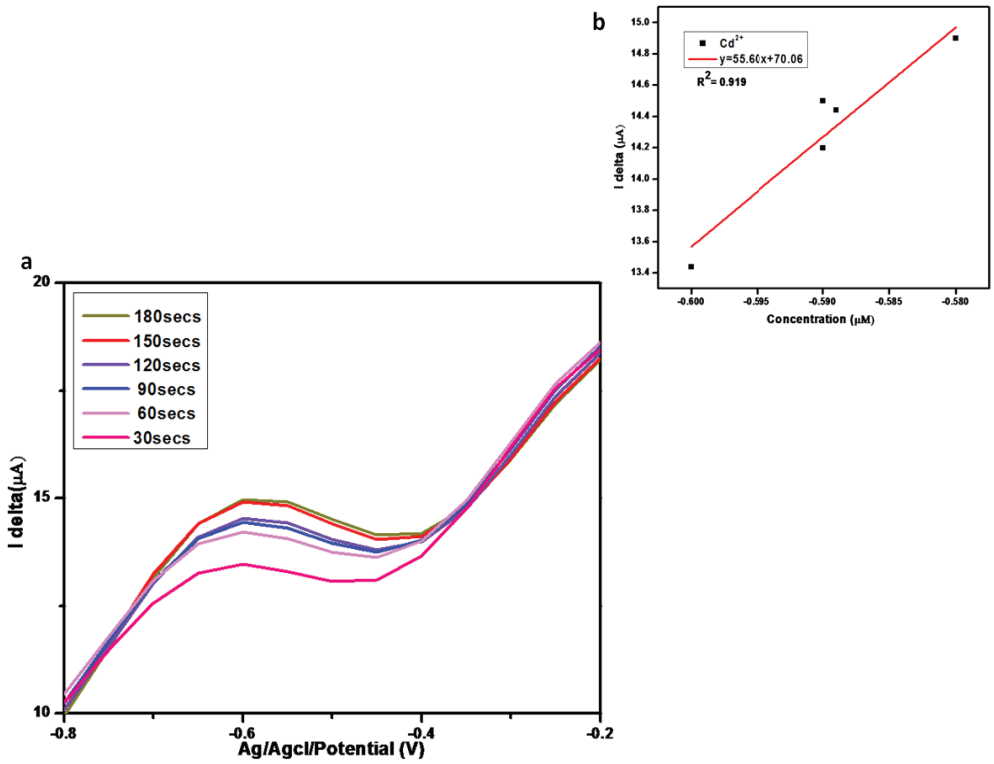

Fig. 6. (a) 0.2 μM concentration of Cd(II) ions in PBS (pH 6) with different accumulation time and (b) linear fitting plot for 0.2 μM concentration.

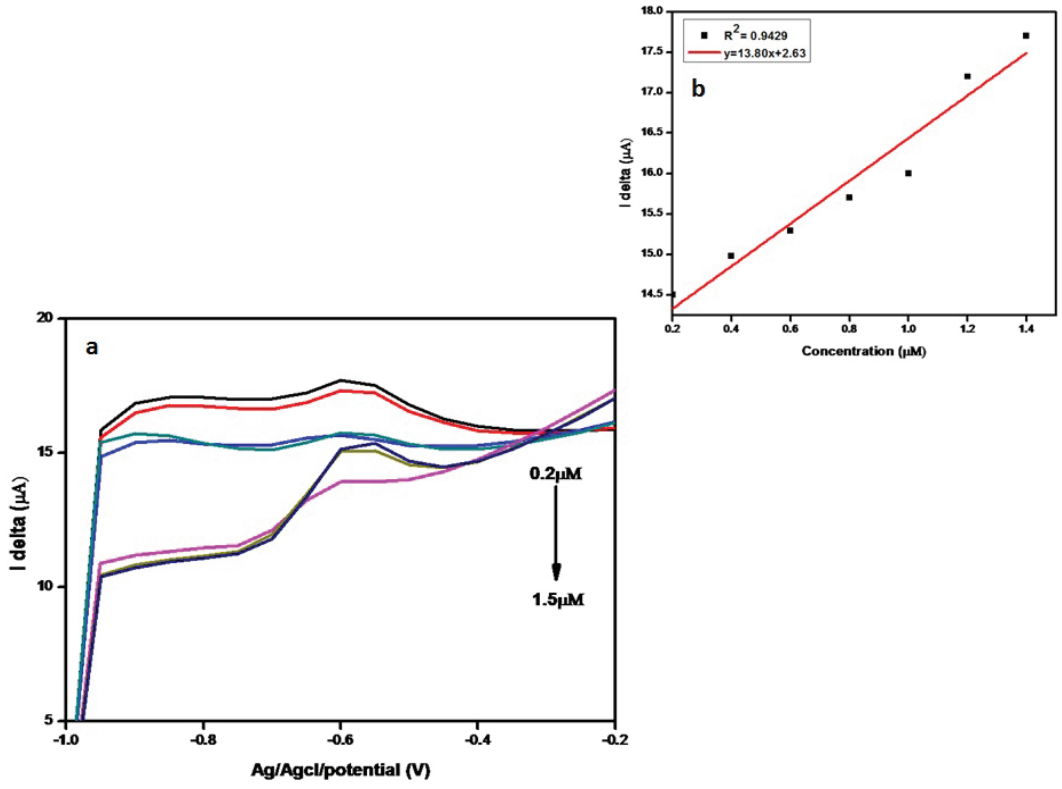

Fig. 7. (a) SWV curves for 0.2–1.5 μM concentrations for Cd(II) and (b) linear fitting plot for different concentrations.

performance to detect Cd(II) ions which was compared with different functionalized NCs as shown in Table 1.

Mechanism behind CA ZnO NC toward the detection Cd(II) ions:

The following mechanism for the behavior of CA functionalized ZnO NC is ascribed as follows:

- There is the fast electron transfer at the electrode surface hindered with attachment of obtained NC due to the high surface area and more number of active sites which made the affinity toward Cd(II) ions.
- Introduction of surface anchoring of polymer (chitosan) on the ZnO NPs increases the electron diffusion toward the electrode surface. This is because the ZnO can form conductivity path for enhancing the diffusion targeting Cd(II) ions.
- It was investigated that, upon increasing the metal ion concentration there was drastic reduction of current peaks because high porous structure which provides disturbance in the system during the electron transport. The mechanism for the behavior has been given in schematic representation in Fig. 8.

3.5.5. Linear range and detection limit

The determination of relationship between current and ionic concentration was obtained using linear curve fitting as shown in Fig. 7(b). The correlation coefficient found to be 0.9429, lowest detection is found to be 1.5 μM and the limit of detection (LOD) was calculated as 1.39 nM for the decreasing current peak with increasing metal ion concentration. The LOD for the obtained electrode material was compared with other materials and it was tabulated in Table 1. From the results, we can see that LOD in the present CA zinc oxide NC Cd(II) electrochemical sensor is comparatively showed satisfactory performance with previously reported sensing materials listed in Table 1.

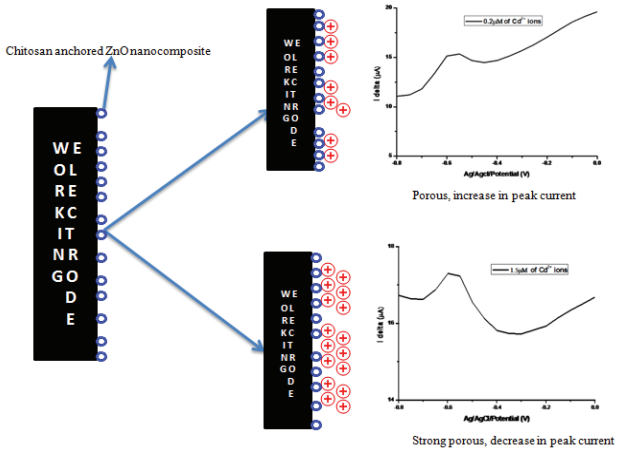

Fig. 8. Schematic representation of mechanism of chitosan anchored ZnO NC and its behavior.

3.5.6. Stability and regeneration of chitosan anchored ZnO nanoparticles glassy carbon electrode

The stability of CA ZnO NPs on GCE in pH 6 medium was inspected. The SWV peak current reaction was measured ceaselessly for 10 d in a progression of aggregation recovery tests. The electrodes were placed away in 0.1 M PBS at pH 6 at room temperature when not being used. The everyday dependability utilization of CA ZnO NC detecting interface was appeared in Fig. 9. For once in every day recoveries, there was a decline in cadmium current of 0.27 for first day, 0.45 for second day and it took after an improper slipping pattern on recovery–collection cycle. The capacity life was additionally been tried by placing away the electrode for 2 d under 5°C in PBS arrangement when not being used. Previously, the present reaction remains practically same; then after the fact stockpiling period. These examinations showed that CA ZnO NC on GCE detecting interface is comparatively stable and can be recovered.

3.6. Determination of Cd(II) on real-time analysis

Chinese cabbage of 1 g was chopped and dissolved in 1 mL of concentrated sulfuric acid and 0.25 mL of hydrogen peroxide was added. All these mixtures are incubated for 8 h and the resulting product was filtered and diluted in 0.1 M of PBS in a volume proportion of 1:1. The feasibility in the real sample was evaluated with different Cd(II) concentrations. As shown in Table 2, the average recoveries in the range from 57% and 70% were obtained in spiked samples, indicating the good accuracy of this proposed method.

Table 2
Results on real-time analysis over Chinese cabbage using electrochemical sensor

S. No.	Cd(II)		Recovery (%)
	Added (μM)	Found (μM)	
1	1.75	1	57.1
2	5	3.5	70

Table 1
A comparative study of various surface functionalized nanocomposites with their current peak responses and their detection limit

S. No.	Materials used	pH	Peak current response (μA)	LOD	References
1	Reduced graphene oxide–Fe_3O_4 nanocomposites	5	42	8 nM	[17]
2	Nafion–graphene nanocomposite film	4.5	36	0.005 μg/L	[18]
3	Chitosan anchored ZnO nanocomposite	6	20	1.39 nM	This work
4	–NH_2 functionalized Si nanowires	4	3.5	0.0035 μA/nM	[19]
5	Nanocomposite incorporated in chitosan matrix	4.5	2	45.2 nM	[20]

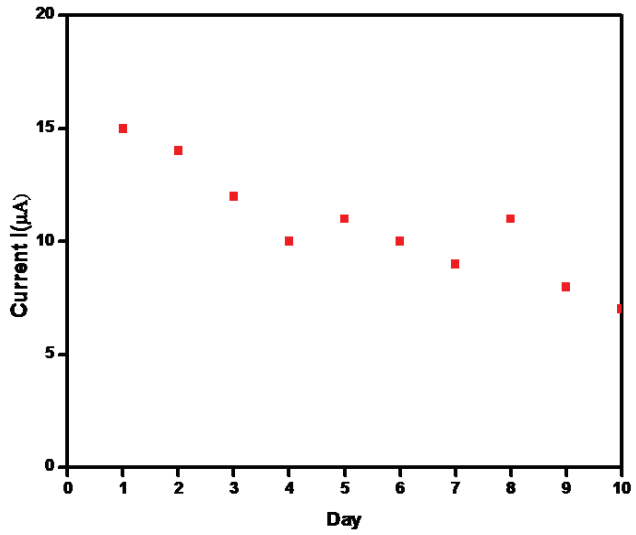

Fig. 9. Daily use stability studies of chitosan anchored ZnO NC on GCE interface, after each measurement Cd(II) ions containing PBS under pH 6 was replaced. Reaccumulation was conducted in same medium with 90 s accumulation time.

4. Conclusion

In summary, chitosan functionalized ZnO NC was synthesized using chemical method. The obtained product was modified with GCE and used as electrochemical sensor for the detection of Cd(II) ions. The acquired product exhibit microporous which was confirmed using BET isotherm analysis. SEM analysis showed that NC was spherical in shape with particle distributed evenly. On investigating the electrochemical behavior of GCE modified electrode, decrease in current peaks with increase in ionic concentration were noticed. Under optimal conditions the electrochemical sensor reveals wide range of detection at 0.2–1.5 μM and low range of detection found to be 1.39 nM. Besides, the reproducibility and stability were also studied with satisfactory results along with real-time analysis.

References

[1] H.R. Rajabi, M. Shamsipur, M.M. Zahedi, M. Roushani, On-line flow injection solid phase extraction using imprinted polymeric nanobeads for the preconcentration and determination of mercury ions, Chem. Eng. J., 259 (2015) 330–337.
[2] H.R. Rajabi, M. Roushani, M. Shamsipur, Development of a highly selective voltammetric sensor for nanomolar detection of mercury ions using glassy carbon electrode modified with a novel ion imprinted polymeric nanobeads and multi-wall carbon nanotubes, J. Electroanal. Chem., 693 (2013) 16–22.
[3] L. Jarup, Hazards of heavy metal contamination, Br. Med. Bull., 68 (2003) 167–182.
[4] G. Aragay, J. Pons, A. Merkoci, Recent trends in macro-, micro-, and nanomaterial-based tools and strategies for heavy-metal detection, Chem. Rev., 111 (2011) 3433–3458.
[5] Y. Wang, S. Gao, X. Zang, J. Li, J. Ma, Graphene-based solid-phase extraction combined with flame atomic absorption spectrometry for a sensitive determination of trace amounts of lead in environmental water and vegetable samples, Anal. Chim. Acta, 716 (2012) 112–118.
[6] R. Golbedaghi, S. Jafari, M.R. Yaftian, R. Azadbakht, S. Salehzadeh, B. Jaleh, Determination of cadmium(II) ion by atomic absorption spectrometry after cloud point extraction, J. Iran. Chem. Soc., 9 (2012) 251–256.
[7] M. Zougagh, A.G. de Torres, J.M. Cano Pavon, Determination of cadmium in water by ICP-AES with on-line adsorption preconcentration using DPTH-gel and TS-gel microcolumns, Talanta, 56 (2002) 753–761.
[8] J. Gong, T. Zhou, D. Song, L. Zhang, Monodispersed Au nanoparticles decorated graphene as an enhanced sensing platform for ultrasensitive stripping voltammetric detection of mercury(II), Sens. Actuators, B, 150 (2010) 491–497.
[9] A. Safavi, E. Farjami, Construction of a carbon nanocomposite electrode based on amino acids functionalized gold nanoparticles for trace electrochemical detection of mercury, Anal. Chim. Acta, 688 (2011) 43–48.
[10] M. Mathew, S. Sureshkumar, N. Sandhyarani, Synthesis and characterization of gold–chitosan nanocomposite and application of resultant nanocomposite in sensors, J. Colloid Interface Sci., 93 (2012) 143–147.
[11] D. Guo, J. Li, J. Yuan, W. Zhou, E. Wang, Nafion film immobilized nano Ag-Hg amalgam glassy carbon electrode used for simultaneous determination of lead, cadmium and copper, J. Electroanal. Chem., 22 (2010) 69–73.
[12] D. Selvakumar, A. Alsalme, A. Alghamdi, R. Jayavel, Reduced graphene oxide paper as bimorphic electrical actuators, Mater. Lett., 191 (2017) 182–185.
[13] M. Velmurugan, S.M. Chen, Synthesis and characterization of porous $MnCo_2O_4$ for electrochemical determination of cadmium ions in water samples, Sci. Rep., 7 (2017) 653–666.
[14] K.M. Zeinu, H. Hou, B. Liu, X. Yuan, L. Huang, X. Zhu, J. Hu, J. Yang, S. Liang, X. Wu, Novel hollow sphere bismuth oxide doped mesoporous carbon nanocomposite material derived from sustainable biomass for picomolar electrochemical detection of lead and cadmium, J. Mater. Chem., 4 (2016) 13967–13979.
[15] M. Fayazi, M.A. Taher, D. Afzali, A. Mostafavi, Fe_3O_4 and MnO_2 assembled on halloysite nanotubes: a highly efficient solid-phase extractant for electrochemical detection of mercury(II) ions, Sens. Actuators, B, 228 (2016) 1–9.
[16] Y.-L. Xie, S.-Q. Zhao, H.-L. Ye, J. Yuan, P. Song, S.-Q. Hu, Graphene/CeO_2 hybrid materials for the simultaneous electrochemical detection of cadmium(II), lead(II), copper(II), and mercury(II), J. Electroanal. Chem., 757 (2015) 235–242.
[17] S. Xiong, B. Yang, D. Cai, G. Qiu, Z. Wu, Individual and simultaneous stripping voltammetric and mutual interference analysis of Cd^{2+}, Pb^{2+} and Hg^{2+} with reduced graphene oxide-Fe_3O_4 nanocomposites, Electrochim. Acta, 185 (2015) 52–61.
[18] J. Li, S. Guo, Y. Zhai, E. Wang, Nafion–graphene nanocomposite film as enhanced sensing platform for ultrasensitive determination of cadmium, Electrochem. Commun., 11 (2009) 1085–1088.
[19] Z. Guo, M.-L. Seol, C. Gao, M.-S. Kim, J.-H. Ahn, Y.-K. Choi, X.-J. Huang, Functionalized porous Si nanowires for selective and simultaneous electrochemical detection of Cd(II) and Pb(II) ions, Electrochim. Acta, 211 (2016) 998–1005.
[20] C.I. Fort, L.C. Cotet, A. Vulpoi, G.L. Turdean, V. Danciu, L. Baia, I.C. Popescu, Bismuth doped carbon xerogel nanocomposite incorporated in chitosan matrix for ultrasensitive voltammetric detection of Pb(II) and Cd(II), Sens. Actuators, B, 220 (2015) 712–719.
[21] E. Salih, M. Mekawy, R.Y.A. Hassan, I.M. El-Sherbiny, Synthesis, characterization and electrochemical-sensor applications of zinc oxide/graphene oxide nanocomposite, J. Nanostruct. Chem., 6 (2016) 137–144.
[22] L. Al-Naamani, S. Dobretsov, J. Dutta, Chitosan-zinc oxide nanoparticle composite coating for active food packaging applications, Innovative Food Sci. Emerg. Technol., 38 (2016) 231–237.
[23] V.C. Nguyen, N.L.G. Nguyen, Q.H. Pho, Preparation of magnetic composite based on zinc oxide nanoparticles and chitosan as a photocatalyst for removal of reactive blue 198, Adv. Nat. Sci. Nanosci. Nanotechnol., 6 (2015) 1–8.
[24] Q. Yuan, Y.P. Zhao, L. Li, T. Wang, Ab initio study of ZnO-based gas-sensing mechanisms: surface reconstruction and charge transfer, J. Phys. Chem., 113 (2009) 6107–6113.

[25] M. Fang, J. Long, W. Zhao, L. Wang, G. Chen, pH-responsive chitosan-mediated graphene dispersions, Langmuir, 26 (2010) 16771–16774.
[26] Y. Zuoa, J. Xu, F. Jiang, X. Duana, L. Lub, H. Xing, T. Yang, Y. Zhang, G. Ye, Y. Yu, Voltammetric sensing of Pb(II) using a glassy carbon electrode modified with composites consisting of Co_3O_4 nanoparticles, reduced graphene oxide and chitosan, J. Electroanal. Chem., 801 (2017) 146–152.
[27] T. Priya, N. Dhanalakshmi, N. Thinakaran, Electrochemical behavior of Pb(II) on a heparin modified chitosan/graphene nanocomposite film coated glassy carbon electrode and its sensitive detection, Int. J. Biol. Macromol., 104 (2017) 672–680.
[28] G.Z. Kyzas, D.N. Bikiaris, Recent modifications of chitosan for adsorption applications: a critical and systematic review, Mar. Drugs, 13 (2015) 312–337.
[29] X. Li, H. Zhou, W. Wu, S. Wei, Y. Xu, Y. Kuang, Studies of heavy metal ion adsorption on Chitosan/Sulfydryl-functionalized graphene oxide composites, J. Colloid Interface Sci., 448 (2015) 389–397.
[30] K.-M. Kim, M.-H. Choi, J.-K. Lee, J. Jeong, Y.-R. Kim, M.-K. Kim, S.-M. Paek, J.-M. Oh, Physicochemical properties of surface charge-modified ZnO nanoparticles with different particle sizes, Int. J. Nanomed., 9 (2014) 41–56.
[31] H. Sivaram, D. Selvakumar, A. Alsalme, R. Jayavel, Enhanced performance of PbO nanoparticles and PbO-CdO and PbO-ZnO nanocomposites for supercapacitor application, J. Alloys Compd., 731 (2017) 55–63.
[32] A.V. Kirthi, A.A. Rahuman, G. Rajakumar, S. Marimuthu, T. Santhoshkumar, C. Jayaseelan, G. Elango, A.A. Zahir, C. Kamaraj, A. Bagavan, Biosynthesis of titanium dioxide nanoparticles using bacterium *Bacillus subtilis*, Mater. Lett., 65 (2011) 2745–2747.
[33] M. Busila, V. Musat, T. Textor, B. Mahltig, Synthesis and characterization of antimicrobial textile finishing based on Ag:ZnO nanoparticles/chitosan biocomposites, RSC Adv., 5 (2015) 21562–21572.
[34] M.J. Chithra, M. Sathya, K. Pushpanathan, Effect of pH on crystal size and photoluminescence property of ZnO nanoparticles prepared by chemical precipitation method, Acta Metall. Sinica (Engl. Lett.), 28 (2015) 394–404.
[35] R. Gayathri, K.P. Gopinath, P. Senthil Kumar, A. Saravanan, Antimicrobial activity of *Mukia maderasapatna* stem extract of jujube seeds activated carbon against gram-positive/gram-negative bacteria and fungi strains: application in heavy metal removal, Desal. Wat. Treat., 72 (2017) 418–427.